Delocalized versus localized unoccupied 5f states and the uranium site structure in uranium oxides and glasses probed by x-ray-absorption near-edge structure

J. Petiau, G. Calas, and D. Petitmaire
Laboratoire de Mineralogie Cristallographique Universités de Paris VI et VII, 4 place Jussieu, 75230 Paris Cédex 05, France

A. Bianconi, M. Benfatto, and A. Marcelli
Dipartimento di Fisica, Università degli Studi di Roma "La Sapienza," I-00185 Roma, Italy
(Received 28 February 1986)

X-ray-absorption near-edge structure (XANES) spectroscopy at the $M_{3,4,5}$ and L_3 edges of uranium and thorium using synchrotron radiation has been used to probe the unoccupied 5f electronic states and local structure of uranium sites in oxides and glasses. The uranium sites in hyperstoichiometric UO_{2+x} ($x \sim 0.25$, $x \sim 0.66$) oxides have been studied. The multiple-scattering resonance in the direction of the linear uranyl group UO_2^{2+} is identified in the L_3 XANES spectra of uranyl nitrate hexahydrate. The localization of unoccupied 5f states in uranium and thorium oxides and glasses has been probed by M_4- and M_5-edge spectra. The presence of narrow 5f localized unoccupied states in Th- and U-containing glasses is indicated by the symmetric sharp white line due to $\underline{3d}5f^{n+1}$ final states. The variable width of the white line indicates that the bandwidth of unoccupied 5f states increases by 4 eV going from glasses to oxides. The presence of 5f components in the U 6d conduction band of oxides, due to hybridization between the U 6d,7s and U5f states is shown by a long asymmetric tail of the white line at its high-energy side extending up to 12 eV. No evidence of many-body effects in XANES spectra, due to the configuration interaction between localized 5f configurations which was observed in mixed-valence rare-earth-metal compounds, has been found in Th and U oxides.

I. INTRODUCTION

The present interest in the actinide compounds is due to the characteristic properties of 5f electrons which are in an intermediate localization regime where the 5f correlation energy is of the same order of magnitude as the 5f-bandwidth.[1,2] Therefore uranium compounds belong to the class of materials with intermediate behavior between the systems (like rare-earth compounds) exhibiting localized electronic properties (like magnetism) and the systems exhibiting delocalized properties (like superconductivity).

In the uranium-oxygen bond theoretical calculations[3–5] predict that 5f electrons enter in the chemical bond with oxygen 2p orbitals in agreement with x-ray-emission experiments.[6,7] However the localization of 5f orbitals is indicated by the value of the electron-electron Hubbard interaction U_{ff} for uranium: $U_{ff} \sim 2$ eV has been predicted theoretically[1] and the value $U_{ff} = 1.5$ eV in intermetallics[2] has been found experimentally. Of particular interest is the question of the localization versus itinerancy of 5f electrons determined by different uranium-oxygen bonding configurations, by different crystalline structures, and by changing the U-U distance. In this work we have investigated 5f localization going from glasses to crystalline oxides.

The most studied between uranium oxides is UO_2, which crystallizes in the fluorite structure with eightfold uranium coordination. The valence band of UO_2 has been investigated by x-ray-photoemission spectroscopy (XPS),[8–12] by ultraviolet-photoemission spectroscopy (UPS),[13] by bremsstrahlung isochromat spectroscopy (BIS),[9,10] by resonant photoemission,[14,15] and by x-ray emission.[6,7]

The band structure of UO_2 (Ref. 16) is similar to that of CeO_2 (Ref. 17). The optical spectrum of UO_2 shows sharp $f \rightarrow f$ transitions over a range from 0 to 2 eV interpreted in terms of localized 5f states.[18] The U 5f localized states are in the 5-eV gap between the O 2p valence and U 6d conduction bands. Photoemission experiments show a narrow (about 2 eV large) band of 5f occupied states at 1.5 eV below the Fermi level and BIS experiments a (6—8)-eV broad band of unoccupied 5f states superimposed on the U 6d conduction band.[9,10]

The open problems concern the hybridization of 5f orbitals with the O 2p or the U 6d,7s orbitals, and the final-state effects in photoemission and core-level spectroscopies which can be very important for localized states, as has been found in rare-earth compounds. The satellites of XPS core-level spectra are a good probe of properties of localized electronic states; therefore a great deal of attention has been paid to the charge-transfer satellite at 7 eV core-level spectra of UO_2.[10,12,19]

The hyperstoichiometric UO_{2+x} oxides have attracted much interest. In the range $0 < x < 0.5$ interstitial oxygens enter in the distorted fluorite-type structure, forming uranium sites with tenfold coordination.[20,21] In the hyperstoichiometric oxides in the range $0.5 < x < 1$ the uranium local structure can be described as being formed by distorted pentagonal bipyramids with two short U—O

bonds and five oxygens on the basal plane.[21] In these oxides different sites with different uranium effective charge have been found.[22]

It is commonly assumed that for uranium coordination number larger than eight, 5f orbitals enter more strongly in the chemical bond, as is shown by the decrease in the intensity of the mostly pure 5f occupied valence band at -1.5 eV.[22]

The variation of the spectrum of charge-transfer satellites in the uranium 4f-core XPS spectra in hyperstoichiometric UO_{2+x} oxides[22–25] has been the object of active interest because it has been shown that it is characteristic of the different uranium bond in these oxides.

Here we report an extensive study of uranium oxides and uranium glasses by x-ray-absorption near-edge structure (XANES). XANES spectroscopy,[26,27] using synchrotron radiation, is a growing method of probing both the electronic unoccupied states and the local structure at a selected site. XANES has been widely used to study localized electronic configurations in mixed-valence rare-earth compounds,[28–31] but only few high-resolution studies have been reported on actinide compounds.[32,33]

According to the Fermi golden rule for optical transitions, the transition rate from a core level to an unoccupied state at energy E can be calculated in **k** space and the measured absorption coefficient $\mu(E) \sim P(E) D_{l'}(E)$, where $P(E)$ is the matrix element and $D_{l'}(E)$ the density of states of selected angular momentum l'. Because of the finite lifetime of the excited photoelectron and the dipole transition rules, XANES spectra probe the unoccupied density of states at the selected absorbing site (local) and that of selected angular momentum l' (partial),[34,35] in agreement with experimental finding.[36] The total absorption cross section can be factored into an atomic part and a part due to the structure of atomic environment, $\alpha(E) = \mu_a(E) \mu_s(E)$. Where the atomic cross section $\mu_a(E)$ has strong resonances, as for the $2p \rightarrow nd$ in transition-metal elements,[36] for $3d \rightarrow nf$ transitions in rare-earth metals,[31,37,38] and in actinides, a strong enhancement of the total cross section is observed at the edge, usually called by the spectroscopical name "white line."

Because of inelastic scattering of the photoelectron and finite core-hole lifetime, only a cluster of finite size is relevant to the determination of the final-state wave function of the photoelectron in the range of tens of eV above the Fermi level, and the spatial distribution of neighboring atoms play the major role in the determination of $\mu_s(E)$ in XANES.[26,27]

It has been demonstrated that the absorption cross section for core transitions can be solved in *real space* using the Green-function approach in the frame of multiple-scattering theory, and good agreement between theory and experiment has been found.[39–41] In this approach the limited mean free path of the photoelectron determines the finite size of the cluster of atoms, with the central absorbing atom considered in the calculation.

The important aspect of the solution of the absorption cross section in real space is that physical aspects determining the unoccupied density of states of condensed matter appear explicitly: the spatial arrangement of neighbor atoms[39–41] and interatomic distances.[42,43] It can be shown[40,41] that XANES spectra are determined by photoelectron multiple-scattering pathways which begin and end at the absorbing site. Where possible[40] the total absorption can be expanded

$$\alpha(E) = \alpha_a(E) \left[1 + \sum_{n=2}^{\infty} \chi_n(E) \right],$$

where $\alpha_a(E)$ is the atomic absorption and $\chi_n(E)$ the contributions of scattering pathways involving the absorbing atom and $(n-1)$-neighbor atoms. In the high-energy extended x-ray-absorption fine-structure (EXAFS) regime only the $\chi_2(E)$ term contributes to $\alpha(E)$. Therefore, XANES can be used as a direct probe of local atomic distribution for local-structure determination in complex systems.[26,39–44]

Here we have used L_3 (and M_3) XANES to identify the local structure of uranium sites. The relationship between uranium structure and XANES spectra has been investigated in uranium oxides UO_{2+x} ($x = 0$, ~ 0.25, and ~ 0.66) and in uranyl nitrate. The multiple-scattering resonance for the photoelectron emitted in the direction of the axis of the uranyl group UO_2^{2+} or along the axis of pentagonal bipyramids is identified.

The transitions to the unoccupied 5f states are enhanced by the atomic resonance in the $3d \rightarrow 5f$ cross section at the $M_{4,5}$ edge of uranium and thorium, giving strong white lines. The high-resolution measurements of the white lines of the M_4 and M_5 edges of uranium and thorium allow one to measure the local density of unoccupied states of selected angular momentum $l' = 3$ (because of selection rule $\Delta l = +1$, neglecting $\Delta l = -1$) and total angular momentum $J' = \frac{5}{2}$ and $\frac{7}{2}$, respectively (because of selection rules $\Delta J = +1$ and $\Delta S = 0$). Therefore the $M_{4,5}$ XANES are a good probe for the measure of the bandwidth of unoccupied 5f states at uranium and thorium sites in oxides and in vitreous compounds.

We have found a symmetric and narrow white line in a Th containing glass due to $\underline{3d}5f^1$ final states and its full width of 3.8 eV determined by experimental broadening gives a measure of the resolution of these measurements. The symmetry of the white line (with no high-energy tail) indicates that 5f states are well localized in glasses.

ThO_2, UO_2, and UO_{2+x} show asymmetric white lines with a long tail on the high-energy side extending up to about 12 eV. A long tail at the high-energy side of the white line appears where 5f orbitals contribute to the U 6d,7s conduction band because of hybridization between U 5f and U 6d,7s orbitals. This effect has been well studied for the palladium L_3 white line in palladium compounds.[27,36] This result shows that U 5f orbitals contribute to the unoccupied U 6d,7s conduction band in oxides up to about 12 eV.

The variation of the width of the localized unoccupied U 5f band going from glasses to crystalline oxides has been deduced from the variation of the half-width of the white line at low energy at the rising edge.

In rare-earth compounds where the 4f bandwidth is smaller than the electron-hole exchange energy, multiplet splitting of atomiclike configurations $\underline{3d}4f^{n+1}$ is observed at $M_{4,5}$ edges.[37,38] Therefore, where 5f states are

localized at atomic level in solids, the appearance of atomiclike multiplets in the $\underline{3d}5f^{n+1}$ excitations at $M_{4,5}$ edges is expected. No multiplets are expected, and they have not been observed here for formally $5f^0$ ions like Th^{4+} or U^{6+} in the studied thorium compounds and in the uranyl system giving $\underline{3d}5f^1$ final states in x-ray absorption. The multiplet splitting for $\underline{3d}5f^3$ final states in UO_2 (Ref. 9) is smaller than the resolution of our measurements; therefore, we cannot resolve multiplet splitting.

Large effects due to multielectrons excitations in the inner-shell photoabsorption appear in mixed-valence rare-earth intermetallic compounds where the correlation energy U is larger than the valence bandwidth W ($U > W$),[28–31,45] or in interatomic intermediate-valent (IIV) insulating oxides like CeO_2, PrO_2,[46–48] and NiO,[49] where U is larger than the charge-transfer gap δE. The picture of the electronic structure of these systems requires the theory of configuration interactions to interpret the multielectron final states in XANES.

Here we show that the XANES spectra of uranium and thorium oxides do *not* show multielectron excitations observed in similar rare-earth-metal compounds. Therefore the spectra of thorium and uranium oxides can be interpreted in the framework of a one-particle approximation as can the spectra of transition metals.

The M_4 spectrum of uranyl nitrate (formally $5f^0$) shows a symmetric white line as narrow as that of glasses showing well-localized unoccupied U $5f$ states. A shoulder at ~ 4 eV higher energy than the white-line maximum in a one-electron picture indicates the $5f$ contribution to a well-resolved U $6d$ conduction band. We discuss the alternative hypothesis on the assignment of this shoulder in the spectrum of uranyl nitrate to mixing between $5f^0$ and $5f^1\underline{L}$ configurations in the ground state of a uranyl group.

II. EXPERIMENT

The spectra were recorded by direct transmission measurements using the synchrotron radiation at Laboratoire pour l'Utilisation du Rayonnement Electromagnétique (LURE) in Orsay emitted by the storage ring DCI. The L and M XANES spectra are in a quite different energy range; therefore, a different experimental setup was used.

The M edges in the (3–4)-keV range were measured in two runs. In the first run the storage ring was operated at an energy of 1.55 GeV (current of 100 mA) and the synchrotron radiation was monochromatized by a "channel-cut" single-crystal Ge(111) asymmetrically cut. In the second run the energy was 1.72 GeV, the monochromator was a double-crystal Si(111), and a double flat reflecting mirror was used to avoid harmonic contamination.

The L edges in the range of 17 keV were measured during dedicated runs at 1.85 GeV and 250 mA using a Si (400) crystal. The instrumental bandwidths are principally determined by the size of the synchrotron source, giving a full width at middle heights ~ 0.7 eV for M edges and ~ 5 eV for L edges. The intrinsic core-level widths determined by core-hole lifetime are[50,51] 3.3 eV for U M_4, 3.2 eV for U M_5, and 3.2 eV for Th M_4, and 7.4 eV for U L_3. The overall energy resolution of observed final states is given by the convolution of instrumental bandwidths with the core-hole bandwidths, and it is estimated to be 3.4 eV at $M_{4,5}$ edges and 9 eV at the L_3 edge.

The predicted core-hole lifetime of the U $3p$ level in Ref. 50 is 14 eV for the U M_3 intrinsic bandwidth. This value is not correct; in fact, the measured M_3 spectrum of uranyl nitrate exhibits at threshold an absorption feature $3p \rightarrow 6d$ with a total bandwidth of 9.2 eV, which is smaller than predicted. Because in this energy range the instrumental resolution is negligible in comparison with the intrinsic width of the transition, and taking into account the broadening of the d final state, the $3p$-core-level width is, at maximum, ~ 9 eV.

III. SAMPLES AND THEIR STRUCTURE

We have studied well-characterized crystalline UO_2 and ThO_2 samples, UO_{2+x} oxides which were close to $x \sim 0.66$ and to 0.25, and two borosilicate glasses.

UO_2 and ThO_2 crystallize in the CaF_2-type structure common to tetravalent rare-earth oxides ($a_0 = 5.47$ Å for UO_2 and $a_0 = 5.60$ Å for ThO_2). The metal ions are eightfold coordinated with U—O bond length $d = 2.37$ Å in UO_2.

The hyperstoichiometric uranium oxides UO_{2+x} ($0 < x < 0.5$) form a fluorite-type crystal like UO_2 with oxygen atoms in excess.[52,53] The additional oxygen atoms go into interstitial positions, forming oxygen vacancies and two types of interstitial oxygens, O′ and O″. The formation of chains of uranium clusters in the ratio 2:2:2 (Ref. 20 and 21) determines the presence of uranium sites with coordination number ten, where there are four normal U—O bonds (2.37 Å), four U—O′ of 2.22 Å, and two U—O″ of 2.30 Å in the chain direction. In these sites there is a contraction of 5% of the average U-O distance compared with that in undistorted regions.

For $x = 0.25$ the crystal structure of U_4O_9 is formed by ordering the 2:2:2 cluster chains in a $4a_0$ superlattice (with a smaller lattice parameter a_0 than in UO_2). The complete unit cell contains 64 additional interstitial oxygen atoms at sites O″, 64 vacancies, 64 intertistial sites at sites O′, and 256 uranium sites.

The mean environment of uranium atoms in hyperstoichiometric oxides in the range $0.6 < x < 1$ can be described as being formed by distorted pentagonal bipyramids of oxygen atoms.[21] For $x = 0.66$ the crystal structure of U_3O_8 is formed.[54] In U_3O_8 there are two types of uranium sites, giving a static mixed-valence system. It can be described as γ-UO_3 crystal structure with oxygen vacancies.

The local structure of uranyl nitrate hexahydrate[55,56] is formed by the uranyl group UO_2^{2+} nearly linear [β(O—U—O) = 177°] with a very short U-O distance. The environment of each uranium atom is completed by six oxygen atoms at distances of 2.40—2.55 Å. Four of them belong to bidentate nitrate groups and two to water molecules. We performed EXAFS measurements[57] at the uranium L_3 edge on this compound; the Fourier analysis shows two well-resolved groups of atoms in the first shell, two oxygen atoms at 1.77 ± 0.02 Å, and six (the fitting gives 5.7) oxygen atoms at 2.4—2.5 Å.

The glasses are boro-silicate glasses (60.9 wt. % SiO_2,

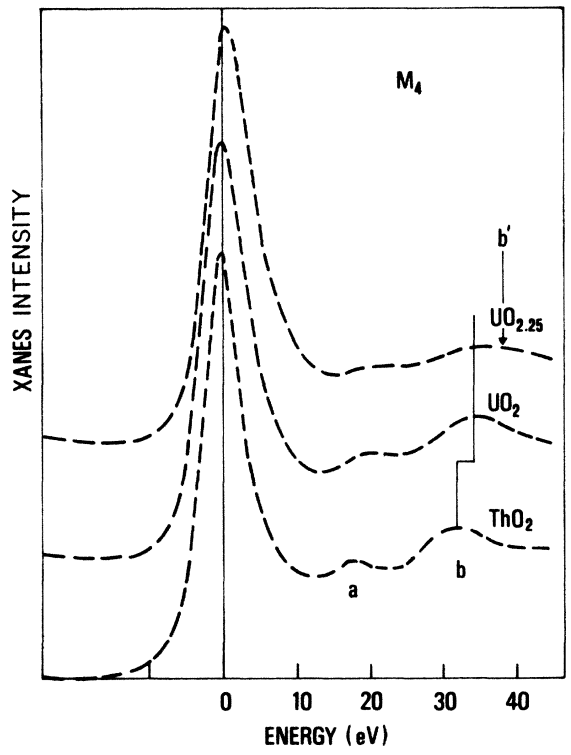

FIG. 1. Thorium and uranium M_4-edge XANES spectra of ThO_2, UO_2, and $UO_{2.25}$. The thorium spectrum has been aligned at the white-line maximum of UO_2.

18.8 wt. % B_2O_3, 13.2 wt. % Na_2O, and 7.1 wt. % UO_2 or ThO_2). This type of glass is a simple model for glasses of technological interest for the stockage of nuclear wastes. EXAFS analysis of this glass indicates that the uranium environment is composed of two oxygen atoms at 1.8 Å and five oxygens at 2.20—2.25 Å, and it will be published in a forthcoming paper.[57] The uranium sites in uranium-containing glasses changes accordingly with composition and preparation conditions; in fact, on other glasses the characteristic short U—O bond of the uranyl group has been found.[58]

IV. RESULTS

A. The $3d \rightarrow 5f$ transitions: The white lines at the $M_{4,5}$ edges

The M_4-edge spectra of ThO_2, and $UO_{2.25}$ are reported in Fig. 1. The threshold is dominated by a white line due to transitions from the $3d$-core level to unoccupied f states. The strong absorption at the white lines is due to the atomic resonance in the $3d \rightarrow 5f$ atomic cross section. The spectra of ThO_2 and UO_2 have been aligned at the white-line maximum. These two spectra are very similar: the full width at half maximum (FWHM) is 7 eV in ThO_2 and 8 eV in UO_2, much larger than the experimental resolution. The white lines are asymmetric as shown in Table I, where the half-width at half maximum (HWHM) on the low- (Γ_1) and high- (Γ_2) energy sides are reported.

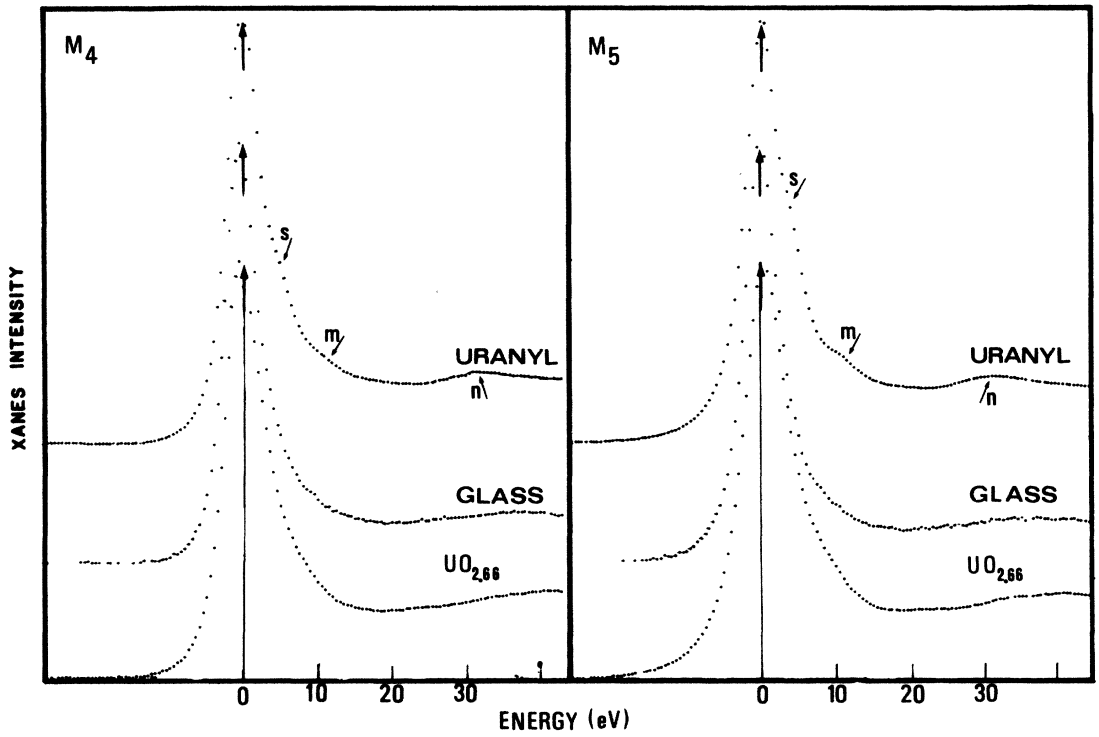

FIG. 2. Uranium M_4-edge (left) and M_5-edge (right) XANES spectra of U_3O_8, uranium-containing borosilicate glass, and uranium nitrate $UO_2(NO_3)+6(H_2O)$.

TABLE I. White-line half widths and energies.

	Thorium glass	ThO_2	UO_2	$UO_{2.25}$	$UO_{2.66}$	Uranyl	Uranium glass
M_4 Γ_1[a]	1.9	2.8	3.0	3.0	2.9	2.6	2.5
M_4 Γ_2[b]	1.9	4.2	5	5	5		3.1
M_5 Γ_1			3	3	3	2.6	2.6
M_5 Γ_2			4.8	4.8	4.5		2.7
M_3 Γ_1			5.6	5.6		4.6	
L_3 Γ_1			6.6	6.6	7.1	5.6	6.2
ΔE (eV)[c]			0.0±0.2	0.8±0.2	1.0±0.2	1.2±0.2	1.0±0.2

[a]Γ_1 half-width at middle height at low-energy side of the white line.
[b]Γ_2 half-width at middle height at high-energy side of the white line.
[c]ΔE is the energy shift of the M_4 (M_5) white-line maxima from the maximum in the M_4 (M_5) spectrum of UO_2.

Taking into account the instrumental bandwidth, we have estimated an overall width of about 7 eV for the unoccupied $5f$ states in the uranium oxide.

In Fig. 2 we report the M_4 and M_5 XANES spectra of $UO_{2.66}$ and of uranium borosilicate glass. The energy position of the white line moves from the energy position in UO_2 toward high energy in hyperstoichiometric oxides, increasing by 0.8±0.2 eV in $UO_{2.25}$ and by 1±0.2 eV in $UO_{2.66}$, as shown in Table I. The maxima of the white lines of $UO_{2.66}$ and of uranium glass in Fig. 2 are at the same energy. These two samples show a large difference in the bandwidth of the white line, as shown in Fig. 3, where the white lines are reported on an enlarged scale. In the uranium glass the white line is nearly symmetric and its bandwidth is only 5.6 eV.

The $M_{4,5}$ spectra of uranyl nitrate are reported in the top panel of Fig. 2 and the M_5 white line is plotted in an expanded scale in Fig. 3. The white line is as narrow as that of uranium glass. In fact, the low-energy side of the two white lines coincide, but the uranyl nitrate shows the shoulder S at 4 eV above the white-line maximum.

In Fig. 4 we report the M_4 white lines of thorium borosilicate glass and ThO_2 and in the left-hand panel the white lines of uranium borosilicate glass and of UO_2. No shift of the energy position of the thorium white line is observed upon going from the oxide to glass. The white line of thorium glass is symmetric and its half-width is only 1.9 eV. An intrinsic width of ~1.0 eV for unoccupied $5f$ states can be deduced. In ThO_2 the half-width Γ_1 of the white line increases to 2.8 eV, showing an increase of 1 eV in the oxide. Moreover, the white line becomes asymmetric, extending up to 12 eV on the high-energy side.

Comparing the white lines of UO_2 and of uranium glass in Fig. 4, we observe the (1±0.2)-eV energy shift due to the increasing effective positive charge of uranium ion in the glass. This shift is similar to the ~1–1.5 eV observed in the core-level shift in XPS spectra going from formal U(VI) to U(IV) ions in oxides.[22–25] The half-width of the white line Γ_1 increases from 2.5 to 3 eV upon going from the glass to UO_2 and becomes more asymmetric.

B. $3d \rightarrow cf$ transitions: Multiple-scattering resonances in the continuum of $M_{4,5}$ XANES

The absorption cross section from the $3d$ inner level to final states in the continuum at energy c in the range 15–50 eV (see Figs. 1 and 2) above the white-line maximum is modulated by multiple-scattering resonances.[39–44] In fact, the atomic cross section $3d \rightarrow cf$ is structureless in this energy region, and therefore the spectral features are determined by the multiple-scattering ma-

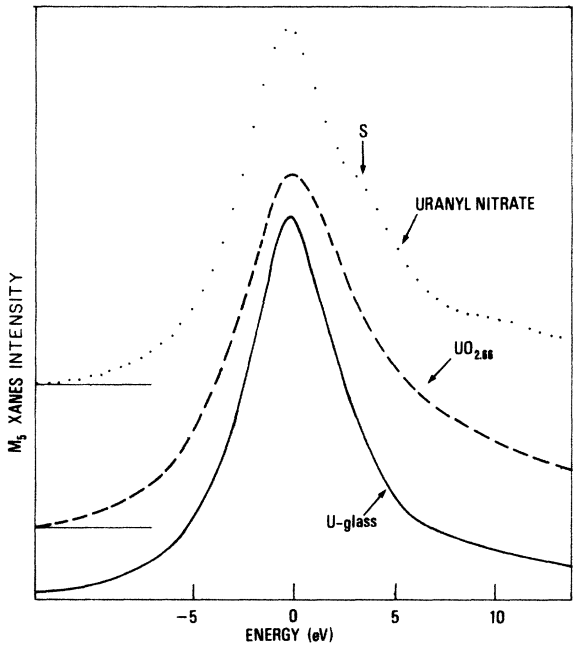

FIG. 3. The white line at the M_5 edge of uranyl nitrate hexahydrate, of $UO_{2.66}$, and of the uranium borosilicate glass are shown from top to bottom. The zero of the energy scale has been taken at the white-line maximum of the spectrum of uranyl nitrate.

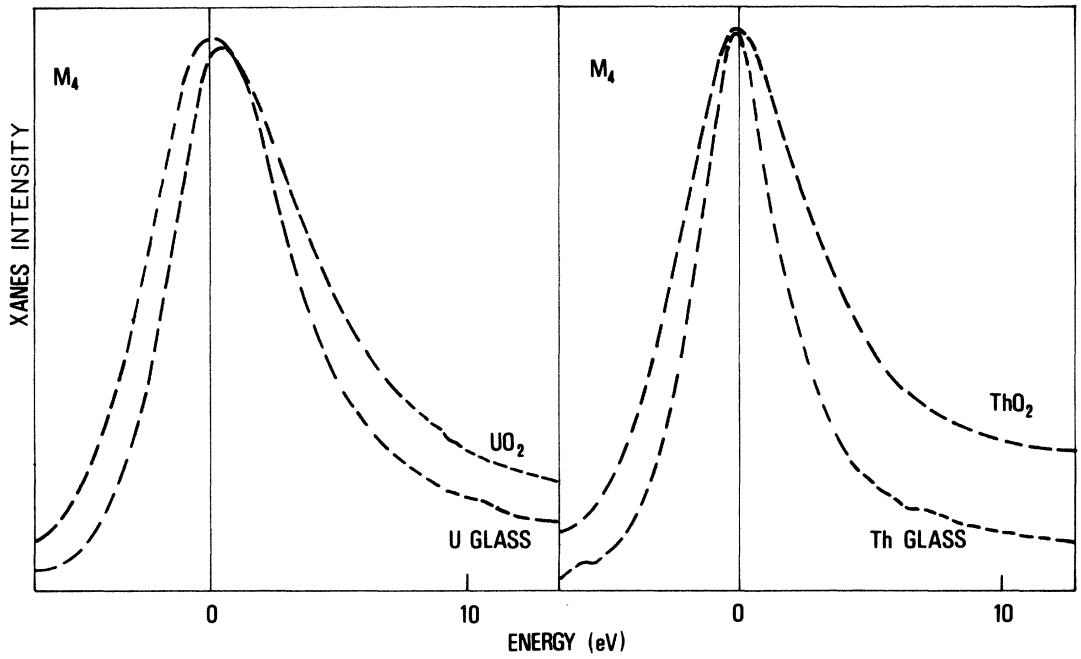

FIG. 4. Comparison between the white lines at M_4-edge spectra of ThO_2 and of the thorium borosilicate glass (right-hand panel). In the left-hand panel the spectra of UO_2 and the uranium borosilicate glass are reported.

trix for an $l'=3$ photoelectron emitted at the uranium site and coming back at the uranium site after multiple-scattering events with neighbor atoms; therefore, the XANES spectra in this energy range can be interpreted in terms of an atomic distribution of neighbor atoms.

The XANES spectra of ThO_2 and of UO_2 in Fig. 1 are very similar, in agreement with the similar fluorite crystal structure. Both spectra show the two peaks a and b. By changing the energy scale of the UO_2 spectrum by a factor $(d_1/d_2)^2=0.95$, where d_1 and d_2 are the U-O distances in UO_2 and the Th-O distance in ThO_2, respectively, we obtain a good overlap between the two spectra. The M_5 XANES of UO_2, $UO_{2.25}$, and $UO_{2.66}$ above the white line are reported in Fig. 5. The final states in the M_5 XANES and in the M_4 XANES are different only for the total angular quantum number J' of the f photoelectron ($J'=\frac{7}{2}$ and $\frac{5}{2}$ at M_5 and M_4, respectively). The zero of the energy scale has been fixed at the maximum of the UO_2 white line. To obtain the spectra in Fig. 5, thick samples were used to enhance the modulations in the range 10—50 eV.

The continuum part of the M_5 spectrum of $UO_{2.25}$ in Fig. 5 (and M_4 in Fig. 1) exhibit the same features as the UO_2 spectrum plus the new feature b'. The feature b' is well resolved in Fig. 5 and it is at ~ 3.8 eV above b. This spectrum can be considered as the sum of the UO_2 spectrum plus a new XANES spectrum determined by the uranium tenfold sites in the 2:2:2 cluster chains formed by interstitial oxygens.

The continuum M_5 XANES spectrum of $UO_{2.66}$ reported in Fig. 5 shows a completely new set of features, Ω and **p**, different from UO_2, which indicate the pentagonal bipyramid uranium-site structure in hyperstoichiometric oxides for $x>0.5$. The spectrum of uranyl nitrate, reported in the top panel of Fig. 2, exhibits a unique XANES spectrum characterized by the satellite s and the multiple-scattering features m and n, which are characteristic of the uranyl UO_2^{2+} site. The continuum M_4 XANES spectrum of uranium borosilicate glass is com-

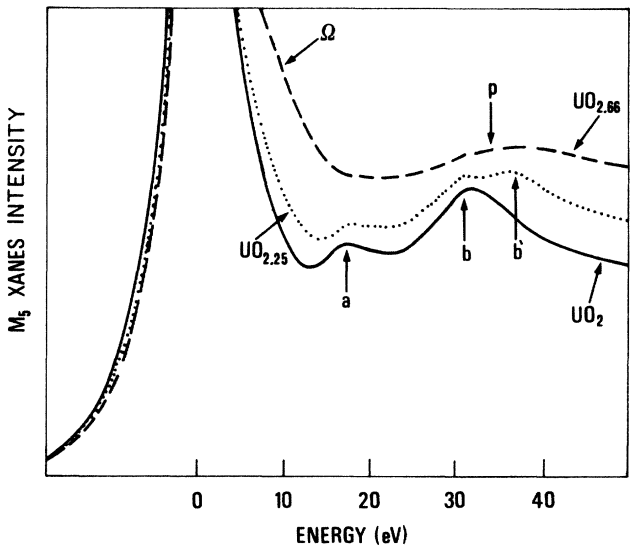

FIG. 5. Uranium M_5-edge XANES spectra of UO_{2+x} ($x=2$, 2.25, and 2.66). Thick samples have been used to put in evidence the modulations of the absorption spectra in the continuum in the range 10—50 eV above the white-line maxima.

pared with $UO_{2.66}$ and uranyl nitrate in Fig. 2. It is clear that the spectra of the glass and of $UO_{2.66}$ are nearly identical.

C. L_3 and M_3 XANES

The uranium L_3 XANES spectra of UO_2, $UO_{2.66}$, and uranyl nitrate are shown in Fig. 6. The spectra show a broad white line, which is determined by the enhancement of the total absorption cross section for transitions to the lowest d-like conduction band by the $2p \rightarrow (6,c)d$ resonance in the atomic cross section [where $(6,c)d$ indicates d-like continuum states c derived by $6d$ atomic orbitals]. In order to study the modulations of the absorption cross section due to structural effects, we have subtracted in each spectrum an arctan curve, shown in Fig. 6, which simulates the spectroscopical absorption jump.

The spectra of UO_2, $UO_{2.66}$, and uranyl nitrate after the subtraction of the arctan are reported in Fig. 7. The M_3-edge spectra have been analyzed in the same way and the difference curves for UO_2 and uranyl nitrate are reported in Fig. 8.

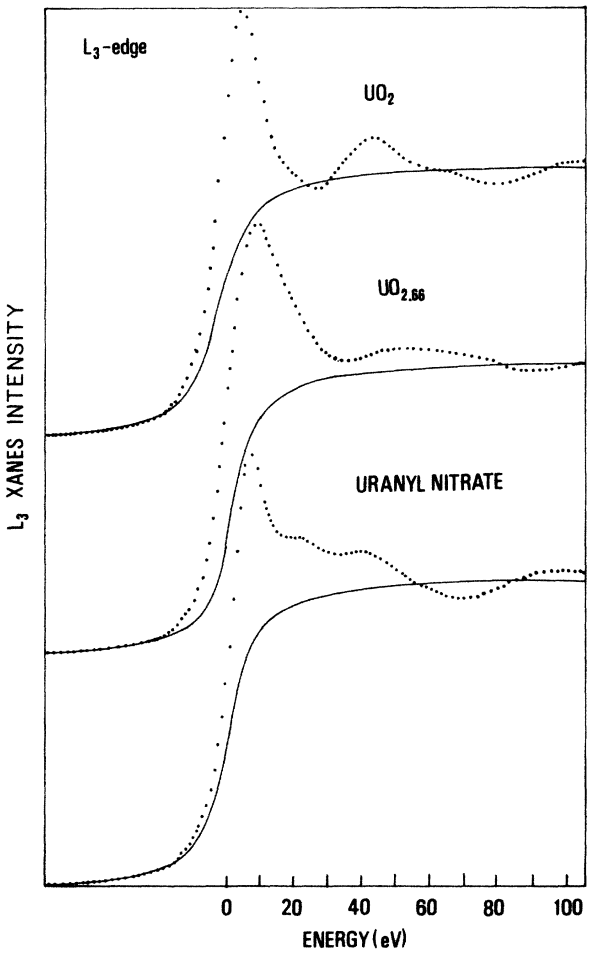

FIG. 6. Uranium L_3-edge XANES of UO_2, U_3O_8, and the uranyl nitrate hexahydrate. The arctan curves for each spectrum simulate the spectroscopic absorption jump.

In Figs. 7 and 8 the results of the fitting of the white lines at threshold with Lorentzian curves are reported. The bandwidth of Lorentzians used to fit the $(6,c)d$ resonance are reported in Table I. The bandwidth of the Lorentzian to fit the uranyl nitrate M_3 white line is only 9.6 eV, well below the reported intrinsic width, 14 eV, of the $3p$-core level, which, therefore, is quite smaller than predicted.[50]

The L_3 XANES spectra of $UO_{2.66}$ and the M_3 and L_3

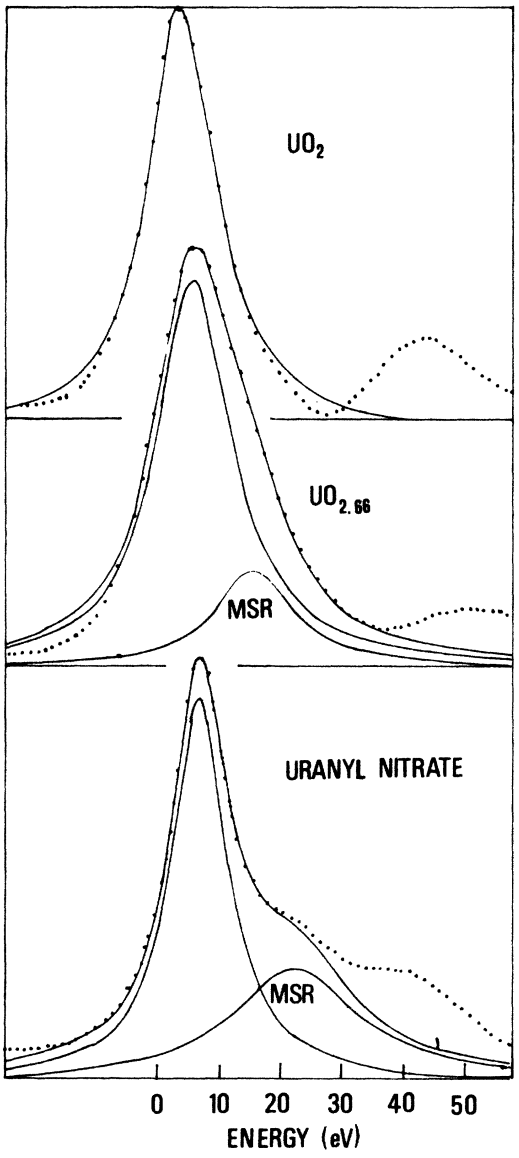

FIG. 7. The difference between the measured L_3 spectra and the arctan curves for each spectrum shown in Fig. 6 are plotted. The results of a fitting with Lorentzian curves of the white lines and of the multiple-scattering resonance (MSR) are plotted. A single line is observed in UO_2. The second Lorentzian is at 15.5 eV in uranyl nitrate. It is a one-electron multiple-scattering resonance in the direction of the short U-O distance characteristic of the uranyl groups. The multiple-scattering resonance in $UO_{2.66}$ at 10 eV above the white line is characteristic of the pentagonal bipyramid groups U_3O_8.

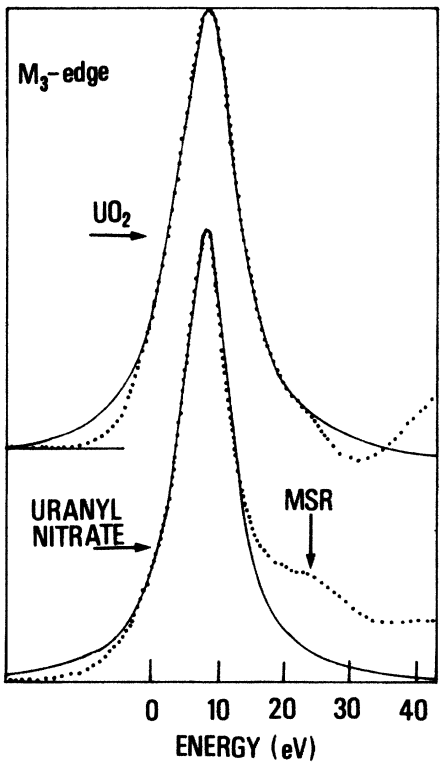

FIG. 8. M_3-edge spectra of UO_2 and uranyl nitrate after subtraction of an arctan curve to simulate the absorption jump. The fitting with a Lorentzian curve of the white lines are shown. The full widths at half maximum are 9.2 eV for uranyl nitrate and 11.3 eV for UO_2. The multiple-scattering resonance (MSR) at 15.5 eV in the spectrum of uranyl nitrate is better resolved in the M_3 spectrum.

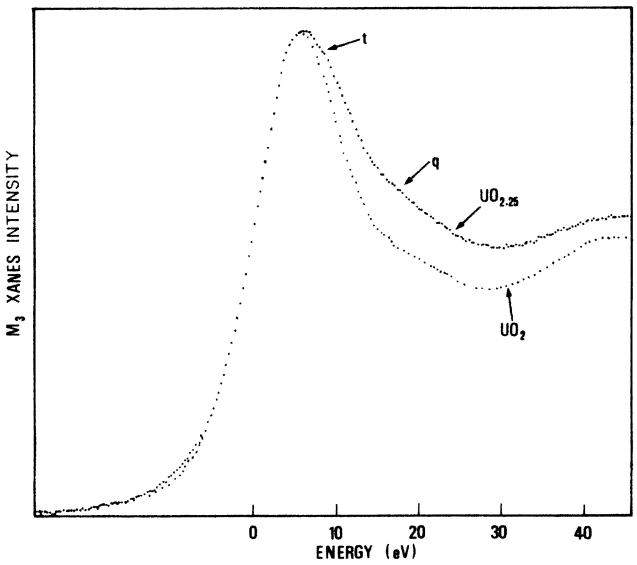

FIG. 9. Uranium M_3-edge XANES of UO_2 and $UO_{2.25}$. The spectra have been aligned on the rising absorption edge and normalized at the absorption maximum to show the differences between the two spectra (features t and q) due to uranium tenfold sites in $UO_{2.25}$.

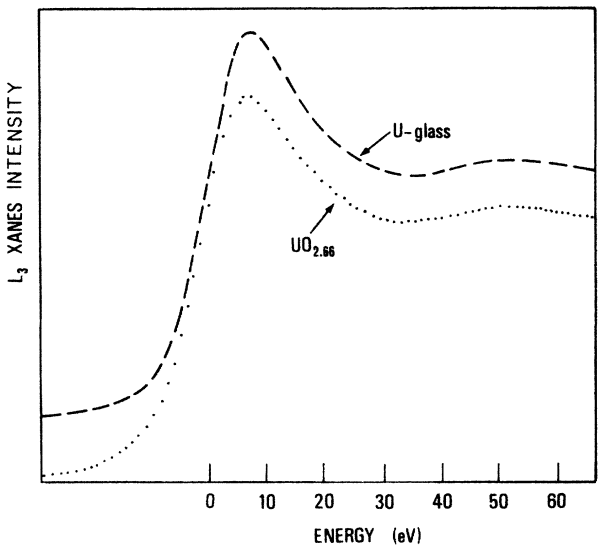

FIG. 10. Uranium L_3 spectrum of the studied uranium borosilicate glass. The L_3 spectrum of $UO_{2.66}$ is reported below for comparison. The spectra are nearly identical, indicating that the uranium site in the glass and in $UO_{2.66}$ is similar.

XANES of uranyl nitrate show a broad strong feature, multiple-scattering resonance (MSR), at 10 and 15.5 eV above the white-line maximum, respectively. The energy positions of these MSR features has been determined by fitting with a second broad Lorentzian, as shown in Fig. 7.

In Fig. 9 we report the M_3-edge spectra of $UO_{2.25}$ compared with that of UO_2 in order to extract the differences between the $UO_{2.66}$ and UO_2 spectra. We show in Fig. 9 the M_3 edge, where we have better resolution than at the L_3 edge. The spectrum of $UO_{2.25}$ shows the same features as UO_2 plus extra features t and q on the high-energy side of the white line. This result is consistent with the $M_{4,5}$ XANES spectra. The extra features t and q are assigned to the tenfold uranium sites in UO_{2+x} ($x<0.5$) oxides. In Fig. 10 we report the L_3 XANES spectrum of the uranium borosilicate glass and of $UO_{2.66}$; the comparison shows the similarity of the two spectra.

V. DISCUSSION

A. The uranium-site structures

The MSR peak in the uranyl nitrate spectrum shown in Fig. 7 can be shown to be determined by multiple scattering in the direction of the linear O-U-O uranyl group. This is shown by comparing the spectrum of uranyl nitrate with the angle-resolved XANES spectra obtained by Templeton and Templeton[32] for the uranyl ion in a single-crystal rubidium uranyl nitrate reported in Fig. 11. The comparison clearly shows that the MSR feature at 15.5 eV above the white line is due to the multiple-scattering resonance of the d photoelectron in the direction x of the short O—U—O bonds of the uranyl ion; in fact, it is present only in the spectrum for the electric field

E polarized along the $\hat{x}$ axis of the linear uranyl ion.

The MSR peak at about 10 eV above the white line in the L_3 spectrum of $UO_{2.66}$ and of the uranium-containing glass are shown in Fig. 7. It determines the long tail on the high-energy side of the L_3 white line, but it is not well resolved as in the uranyl nitrate spectrum. It is characteristic of the sites formed by distorted pentagonal bipyramids where the differences between the shortest and longest U—O bond lengths are 0.4 Å or less, and not 0.7 Å as in the uranyl nitrate, in agreement with EXAFS data.

The tenfold uranium sites along the 2:2:2 cluster chains formed by interstitial oxygens in $UO_{2.25}$ oxide[20,21] have been identified by $M_{4,5}$ and L_3 edges. In the $M_{4,5}$ edges the multiple-scattering feature b moves with the interatomic distance.

It has been demonstrated that the energy of full multiple-scattering resonances for molecular groups of the same symmetry are dependent on the interatomic distance.[42,43] The energy separation E of a multiple-scattering resonance in the continuum from an atomiclike resonance at threshold (like a white line) follows the rule $Ed^2 \sim$const, where d is the interatomic distance. Deviations from this rule are expected for variations of interatomic distances larger than 10%, because the energy dependence of scattering phase shifts cannot be neglected.

The change of the energy E_b of the multiple-scattering peak b in Fig. 1 from ThO_2 to UO_2 is in agreement with the contraction of interatomic distance

$$E_b(ThO_2)/E_b(UO_2)=[d(U—O)/d(Th—O)]^2=0.95 .$$

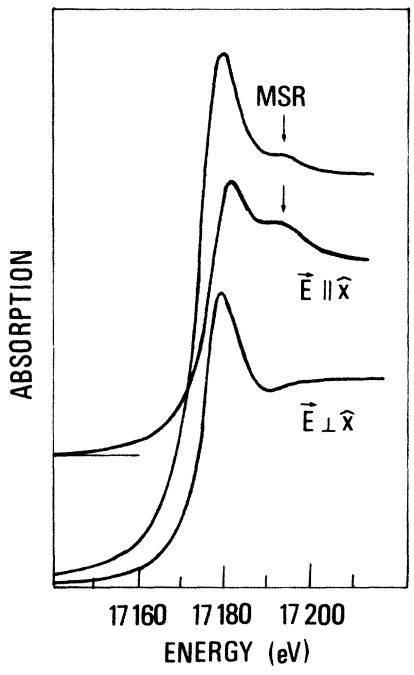

FIG. 11. The L_3 absorption spectrum of uranyl nitrate (upper curve) compared with the polarized spectra of rubidium uranyl nitrate measured by Templeton and Templeton (Ref. 32) for the polarization vector **E** along the uranyl axis **x**, **E**||**x**, and **E**⊥**x** lower curves.

The peak b' in the spectrum of $UO_{2.25}$ in Fig. 5 is assigned to tenfold uranium sites formed by interstitial oxygens. The peak b of $UO_{2.25}$, which coincides with the peak b of UO_2, is due to undistorted eightfold uranium sites. The energy separation between b and b' indicates a contraction of about 5% of the interatomic distance in the tenfold sites. This is in agreement with crystallographic results.[20,21]

The energy shift and shape of the white lines in L_3-edge spectra are essentially due to local-structure effects. This is demonstrated by the angular dependence of the L_3 white line for the uranyl group as shown in Fig. 11. The energy shift of the L_3 white-line maxima in $UO_{2.66}$ and in uranium borosilicate glass from the UO_2 white-line maximum, $\Delta E = 3$ eV, is mainly determined by the contraction of the average uranium-oxygen distance.[43] In fact, the contribution to the edge shift due to variation of core-level binding energies is about 1 eV, as shown by $M_{4,5}$ edges and core-level photoemission.

B. Unoccupied 5*f* states

1. *UO_2 and ThO_2*

The band structure of UO_2 is formed by a bonding valence band V_1 extending between 3 and 8 eV below the Fermi level E_F (mostly formed by O $2p$ orbitals), partially occupied states V_2 (mostly formed by U $5f$ orbitals), and an unoccupied conduction band C_3 (mostly formed by U $6d,7s$ orbitals).

Optical data give evidence of localized $5f$ behavior.[18] Photoemission spectra show a mostly pure f band with negligible dispersion at -1.5 eV below the Fermi level.[9–15] A gap of about 2 eV from f states to the conduction band C_3 was deduced from optical reflectivity. A gap of 5 eV between the V_1 and C_3 bands is in good agreement with photoemission and BIS data[10,59] and band-structure calculations.[16,4,60]

In ThO_2 the localized Th $5f$ band is empty, this has been shown by photoemission data and it is expected to be at higher energy above the O $2p$ valence band, from theoretical calculations.[4]

The open problem concerns the *degree* of the localization of $5f$ states i.e., the degree of mixing of $5f$ orbitals with O $2p$ and U $6d,7s$ orbitals. The mixing of U $5f$ with O $2p$ orbitals has been the object of several investigations and discussions by Naegele *et al.*[9] but in any case the contribution of U $5f$ orbitals to the O $2p$ valence band is small, as is shown by the resonance photoemission of the broad O $2p$ valence band V_1.[14,15]

Here we discuss the evidence of mixing of the U $5f$ and U $6d,7s$ orbitals in the unoccupied conduction band. In the BIS spectrum of UO_2 the strong and broad peak extending from 2 to 8 eV above E_F has been demonstrated to be due to $5f$ final states[59] and was assigned to $5f^3$ final states.[10] The explanation of the broadening of this peak remain unsolved. The multiplet splitting for $5f^3$ final states is expected to be much smaller[9,61] than the width of the broad line assigned to the $5f^3$ final states in BIS spectra. In the XANES spectra the energy resolution of 3.5 eV does not allow one to resolve the $3d5f^3$ multiplets.

In order to extract information on the unoccupied 5f states from the $M_{4,5}$ white line, we start the interpretation of the thorium glass and ThO_2. In this case the final states are $\underline{3d}5f^1$ and no multiplets are present. The symmetric white line in the glass—as large as the intrinsic overall resolution determined by the core-hole lifetime—indicates that the lowest unoccupied band is a narrow (less than 1 eV wide) band formed by localized 5f states. Going from the thorium-containing glass to ThO_2, the energy position of 5f states remains constant; in agreement with the fact that the formal valence of thorium is the same. In the glass, the full width is much narrower (3.8 eV) than in ThO_2 (7 eV). This indicates the formation of a broad band of 5f unoccupied states in ThO_2. The variation of the width of localized 5f unoccupied states at the bottom of the conduction band is indicated by the variation of the half-width at the low-energy side Γ_1 of the $M_{4,5}$ white lines from the value of 1.9 eV for Th-containing glass to 2.8 eV in ThO_2.

The other difference between the glass and the oxide is the long tail on the high-energy side of the oxide, which indicates that the 5f orbitals contribute to the conduction band of ThO_2, extending at higher energy up to about 12 eV. Therefore, we can conclude that in Th-containing glass the 5f states are all confined in a narrow band, while in ThO_2 there is an important hybridization between 5f and 6d,7s orbitals in the broad conduction band.

The similarity between the $M_{4,5}$ spectra of ThO_2 and of UO_2 indicates that also in UO_2 there is a large mixing of U 5f and U 6d,7s orbitals. The full bandwidth, ~ 8 eV, of the 3d-core excitation to the unoccupied 5f states in UO_2 has been found to be much larger than that determined by instrumental resolution and therefore cannot be assigned to unresolved multiplets. The intrinsic full width of the unoccupied 5f states in UO_2, ~ 7 eV, extracted from XANES, is in agreement with the width of the unoccupied 5f band detected by BIS.[7,10]

Comparing the uranium M_4 spectra of uranium metals measured by Lawrence *et al.*[33] with the spectra of oxides and glasses measured here, we observe that the asymmetry of the $M_{4,5}$ white line in the metals is larger than in the oxides. The full widths of the M_5 white line in UMn_2 and UAl_2 are 10.2—10.8 eV, and are therefore larger than in the oxides studied here. The half-width at the high-energy side, Γ_2, is 1.9 eV in the thorium-containing glass, 4.2 eV in ThO_2, and 5 eV in UO_2, as reported in Table I and about 6.5 eV in metals obtained from the figures in Ref. 33. This long tail of 5f states in the conduction band in the oxides is due to an increasing contribution of f orbitals to a higher-energy conduction band extending up to 12 eV.

The observed broadening of the unoccupied f bands going from a glass to a crystalline oxide is similar to that observed for the unoccupied 3d band of palladium going from Pd impurities to crystalline oxide PdO.[62] A similar asymmetry of the white line has been found in the L_3 edge of Pd metal. The observed asymmetry of the white line in Pd metal has been clearly demonstrated to be determined by the atomic cross section enhancing the d, components in the sp conduction band extending up to 8 eV, while the unoccupied 4d states, are confined in a narrow set of states which correspond to the maximum of the white line.[27,36,62]

The behavior of core transitions to 5f states is different from that observed in rare-earth compounds, where the bandwidth of the core transitions to unoccupied atomic-like 4f states is nearly constant in different systems.

Comparing the M_4 and L_3 spectra of ThO_2 and UO_2 with the M_4 (Refs. 63 and 64) and L_3 (Ref. 48) spectra of CeO_2, which has the same crystallographic structure and similar electronic band structure,[16,17] the spectra of actinide oxides do not show the multielectron final states observed in CeO_2. The presence of multielectron final states in CeO_2 has been shown to be due to configuration interaction between the $4f^0$ and $4f^1\underline{L}$ ($\underline{L}$ indicates a hole in the O 2p band) configurations separated by ΔE in the ground states.[47,49] The presence of configuration interaction in the ground state in insulating oxides is determined by the large correlation energy $U_{ff} \sim 8$ eV for 4f states that becomes larger than the charge-transfer gap δE to excite an electron from the O 2p band to the unoccupied 4f localized states, which is about 4 eV in CeO_2. Moreover the hybridization energy V between O 2p and 4f orbitals is of the same order of magnitude of the energy separation between the two many-body configurations ($V \sim \Delta E$).

The fact that no mixing of configurations is observed in UO_2 indicates that in spite of non-negligible correlation energy U_{ff} for 5f states ($U_{ff} \sim \delta E$), we are in the case of integral valence.[48] This corresponds to the condition $V \ll \Delta E$, when the hybridization between U 5f and O 2p is negligible with respect to the energy difference between f^{n+1} and f^n many-body configurations.

2. UO_{2+x} and the uranium borosilicate glass

The bandwidth of unoccupied 5f states in UO_{2+x} is the same as in UO_2. We do not observe the static mixed valence associated with different sites in hyperstoichiometric oxides. We observe a unique shift of about 0.7 eV upon going from UO_2 to $UO_{2.25}$, which is in agreement with the XPS shift of the 4f core lines.[24,25] This indicates that the shift can be associated with the variation of the core-level binding energy, and the energy position of unoccupied 5f states remains nearly constant.

The fact that we see a small shift as in XPS indicates that the decrease of localized 5f electrons in the V_2 band observed in the XPS valence-band spectrum in $UO_{2.25}$ does not affect the position of unoccupied conduction band.

In the $UO_{2.66}$ oxide we observe a shift of about 1.1 eV which is as large as that observed in 4f-level core-level photoemission[22,23] and indicates the formation of sites with formal valence U^{6+}. The bandwidth of the unoccupied 5f band at the M_4 edge is similar to that of UO_2.

Comparing the M_4 white lines in $UO_{2.66}$ an in the borosilicate glass, we observe that the energy position of the white-line maxima coincide, showing the same uranium effective charge. The only difference between the XANES spectra of these compounds is the narrowing of the M_4 and M_5 white lines in the glass. This comparison clearly shows the broadening of unoccupied 5f bandwidth by about a factor of 2 from the glass to the oxide.

In conclusion, we have found that in the hyper-

stoichiometric oxides the bandwidth of unoccupied $5f$ states and the hybridization between U $5f$ and U $6d,7s$ remains constant within the experimental resolution.

The presence of different sites in $UO_{2.66}$ with U^{4+} and U^{6+} formal charge was detected by core-level XPS spectra, which show two peaks separated by 1 eV,[22,23] and in the uranium-containing glass, where the optical spectra indicate U^{5+} and U^{6+}. The presence of different sites with different formal charge is not detected by XANES showing that the energy separation of final states $\underline{3d}5f^1$, $\underline{3d}5f^2$, or $\underline{3d}5f^3$ is not larger than 1 eV, as found in XPS. If the $5f$ occupation number in these oxides were an integer and if the correlation energy were $U_{ff}=4.6$ eV as suggested in Ref. 10, the Coulomb interaction between the $\underline{3d}$-core hole and the $5f$ electron should be larger than 4.6 eV and therefore we should be able to separate the final states with an experimental resolution of 3.5 eV.

C. Uranyl nitrate

The M_4 spectrum of uranyl nitrate in Fig. 3 shows a narrow white line due to the $\underline{3d}5f^1$ final state at threshold. The narrow bandwidth of unoccupied $5f$ states indicates that they are well localized, as in the Th-containing glass.

The M_4 spectrum of uranyl nitrate exhibits a shoulder s at about 4 eV above the white-line maximum which is not present in glasses. Following the above discussion, we assign this shoulder to the f components of the U $6d,7s$ conduction band. The characteristic spectrum of uranyl is determined by the fact that the unoccupied $5f$ localized band is more localized than in uranium oxides and separated from the U $6d$ conduction band; however, an important hybridization between U $5f$ and U $6d,7s$ orbitals is expected, as indicated by theoretical calculations.[4,5]

The theoretical calculations of the electronic structure of uranyl compounds also show a large mixing of U $5f$ and O $2p$ orbitals.[5] The U $5f$ states at -1.5 eV in UO_2 are not present in the valence-band photoemission spectra of uranyl compounds.[22] The optical spectrum of uranyl nitrate does not show $f\rightarrow f$ transitions and shows a charge-transfer gap at about 3 eV (Ref. 65) that can be assigned to the transition from the mostly oxygen $2p$ band to the unoccupied U $5f$ states. The core-level XPS spectra show a characteristic satellite at 3.9 eV from the main $4f$ line,[66] as do other uranyl compounds[67] and U(VI) oxides.[22] Keller and Jorgensen[67] pointed out the need for an explanation of this satellite different from that of other satellites of uranium oxides.

Here we discuss the hypothesis that the shoulder at 4 eV at the M_4 edge is due to a charge-transfer excitation of a valence electron. In uranyl nitrate the $5f$ states are more localized and the charge-transfer gap δE (O $2p\rightarrow$U$5f$) ~ 3 eV is close to the U_{ff} correlation energy ~ 2 eV.[1,2] Therefore, using the language of configuration interaction a mixing of the localized configuration $5f^0$ and $5f^1\underline{L}$ can be expected, as in CeO_2 and NiO,[46–49] that we call interatomic intermediate-valence (IIV) systems, if the hybridization energy V also becomes larger than the energy separation of the two configurations. Where this hypothesis will be verified, the 4-eV satellite in the M_4 XANES can be associated with the final state $\underline{3d}\,\underline{L}5f^2$ and the main line with the $\underline{3d}5f^1$ final state. The large intensity of the satellite in XANES can be explained by mixing of $5f^0$ and $5f^1\underline{L}$ configurations in the ground state, in agreement with the expected large covalence of the uranium-oxygen bond in uranyl UO_2^{2+} groups.

ACKNOWLEDGMENTS

We thank the staff of Laboratoire pour l'Utilisation du Rayonnement Electromagnétique (LURE), Orsay, France, for operating the synchrotron-radiation facility and for development of x-ray instrumentation. We are indebted to the Centre d'Etudes Nucléaires de-Marcoule for the elaboration of the glass. We thank G. C. Allen and A. Kotani for many stimulating discussions.

[1] J. F. Herbst, R. E. Watson, and I. Lindgren, Phys. Rev. B **14**, 3265 (1976).
[2] J. W. Allen, S. J. Oh, L. E. Cox, W. P. Ellis, M. S. Wire, Z. Fisk, J. L. Smith, B. B. Pate, and A. J. Arko, Phys. Rev. Lett. **54**, 2635 (1985).
[3] L. E. Cox, J. Electron Spectrosc. Relat. Phenom. **26**, 167 (1982).
[4] V. A. Gubanov, A. Rosen, and D. E. Ellis, Solid State Commun. **22**, 219 (1977).
[5] V. Heera, G. Seifert, and P. Ziesche, Phys. Status Solid B **118**, K107 (1983); **119**, K1 (1983).
[6] C. Bonnelle and G. Lachere, J. Phys. (Paris) **35**, 295 (1974); and J. Phys. (Paris) Colloq. **41**, C5-15 (1980).
[7] C. Bonnelle, Struct. Bonding (Berlin) **31**, 23 (1976).
[8] B. W. Veal and D. J. Lam, Phys. Rev. B **10**, 4902 (1974).
[9] J. R. Naegele, J. Ghijsen, and L. Manes, Struct. Bonding (Berlin) **59/60**, 197 (1985).
[10] Y. Baer and J. Shoenes, Solid State Commun. **33**, 885 (1980).
[11] H. Grohs, H. Hochst, P. Steiner, S. Hufner, and K. H. J. Bushow, Solid State Commun. **33**, 573 (1980).
[12] W. D. Schneider and C. Laubschat, Phys. Rev. Lett. **46**, 1023 (1981); Phys. Rev. B **23**, 997 (1981).
[13] P. R. Norton, R. L. Tapping, D. K. Creber, and W. J. L. Buyers, Phys. Rev. B **21**, 2572 (1980).
[14] B. Reihl, N. Martenson, D. E. Eastman, A. J. Arko, and O. Vogt, Phys. Rev. B **26**, 1842 (1982).
[15] B. Reihl, M. Domke, G. Kaindl, G. Kalkowski, C. Laubschat, F. Hullinger, and W. D. Schneider, Phys. Rev. B **32**, 3530 (1985).
[16] P. J. Kelly and M. S. S. Brooks, J. Phys. C **13**, L939 (1980).
[17] D. D. Koelling, A. M. Boering, and J. H. Wood, Solid State Commun. **47**, 227 (1983).
[18] J. Shoenes, Phys. Rep. **63**, 301 (1980).
[19] L. E. Cox, W. P. Ellis, R. D. Cowan, J. W. Allen, and S. J. Oh, Phys. Rev. B **31**, 2467 (1985).
[20] G. C. Allen, P. A. Tempest, and J. W. Tyler, Nature (London) **295**, 48 (1982).
[21] G. C. Allen and P. A. Tempest, J. Chem. Soc. Dalton Trans. **1982**, 2169; **1983**, 2673.
[22] Yu. A. Teterin, V. M. Kulakov, A. S. Boer, N. B. Nevzorov, I. V. Melnikov, L. V. Mashirov, D. N. Suglobov, and A. G. Zelenkov, Phys. Chem. Miner. **7**, 151 (1981).

[23]J. J. Pireaux, J. Riga, E. Thibaut, C. Tenret-Noel, R. Caudano, and J. J. Verbist, Chem. Phys. **22**, 113 (1977).
[24]G. C. Allen J. A. Crofts, M. T. Curtis, P. M. Tucker, D. Chadwick, and P. J. Hampson, J. Chem. Soc. Dalton Trans. **1974**, 1296.
[25]G. C. Allen, P. M. Tucker, and J. W. Tyler, J. Phys. Chem. **86**, 224 (1982).
[26]A. Bianconi, Appl. Surf Sci. **6**, 392 (1980).
[27]A. Bianconi, in *X-Ray Absorption: Principles and Techniques* of *EXAFS, SEXAFS and XANES,* edited by R. Prinz and D. Konigsberger (Wiley, New York, 1987).
[28]G. Krill, J. P. Kappler, A. Meyer, L. Abadli, and M. Ravet, J. Phys. F **11**, 17 (1981).
[29]A. Bianconi, S. Modesti, M. Campagna, K. Fisher, and S. Stizza, J. Phys. C **14**, 4737 (1981).
[30]J. Rohler, D. Wohlleben, J. P. Kappler, and G. Krill, Phys. Lett **103**A, 220 (1984).
[31]G. Kaindl, W. D. Brewer, G. Kalkowski, and F. Holtzberg, Phys. Rev. Lett. **51**, 2056 (1983).
[32]D. H. Templeton and L. K. Templeton, Acta Crystallogr. Sect. A **38**, 62 (1982).
[33]J. M. Lawrence, M. L.den Boer, R. D. Parks, and J. L. Smith, Phys. Rev. B **29**, 568 (1984).
[34]P. A. Papaconstantopoulos, D. J. Nagel, and C. Jones-Bjorklund, Int. J. Quant. Chem. Symp. **12**, 497 (1978).
[35]J. E. Muller and J. W. Wilkins, Phys. Rev. B **29**, 4331 (1984).
[36]M. Benfatto, A. Bianconi, I. Davoli, L. Incoccia, S. Mobilio, and S. Stizza, Solid State Commun. **46**, 367 (1983).
[37]J. M. Esteva, R. C. Karnatak, J. C. Fuggle, and G. A. Sawatzky, Phys. Rev. Lett. **50**, 910 (1983).
[38]B. T. Thole, G. van der Laan, J. C. Fuggle, G. A. Sawatzky, R. C. Karnatak, and J. M. Esteva, Phys. Rev. B **32**, 5107 (1985).
[39]A. Bianconi, M. Dell'Ariccia, P. J. Durham, and J. B. Pendry, Phys. Rev. B **26**, 6502 (1982).
[40]M. Benfatto, C. R. Natoli, A. Bianconi, J. Garcia, A. Marcelli, M. Fanfoni, and I. Davoli, Laboratori Nazionali di Frascati Report No. LNF-85/26(P), 1985 (to be published).
[41]A. Bianconi, J. Garcia, A. Marcelli, M. Benfatto, C. R. Natoli, and I. Davoli, J. Phys. (Paris) Coloq. **46**, C9-101 (1985).
[42]A. Bianconi, M. Dell'Ariccia, A. Gargano, and C. R. Natoli, in *EXAFS and Near Edge Structure,* Vol. 27 of *Springer Series in Chemical Physics,* edited by A. Bianconi, L. Incoccia, and S. Stipcich (Springer, Berlin, 1983), p. 51.
[43]A. Bianconi, E. Fritsch, G. Calas, and J. Petiau, Phys. Rev. B **32**, 4292 (1985).
[44]A. Bianconi, A. Congiu-Castellano, P. J. Durham, S. S. Hasnain, and S. Philips, Nature (London) **318**, 685 (1985).
[45]J. C. Fuggle, F. V. Hillebrecht, J. M. Esteva, R. C. Karnatak, O. Gunnarson, and K. Schönhammer, Phys. Rev. B **27**, 4637 (1983).
[46]A. Bianconi, A. Marcelli, M. Tomellini, and I. Davoli, J. Magn. Magn. Mater. **47&48**, 209 (1985).
[47]T. Jo and A. Kotani, Solid State Commun. **54**, 451 (1985).
[48]A. Bianconi, A. Marcelli, H. Dexpert, K. Karnatak, A. Kotani, T. Jo, and J. Petiau, Phys. Rev. B (to be published).
[49]I. Davoli, A. Marcelli, A. Banconi, M. Tomellini, and M. Fanfoni, Phys. Rev. B **33**, 2979 (1986).
[50]W. Bambynek, R. Crasemann, R. W. Fink, H. V. Freund, H. Mark, C. D. Swift, R. E. Price, and R. Venugopale Mao, Rev. Mod. Phys. **44**, 716 (1976).
[51]M. O. Krause and J. H. Olivier, J. Phys. Chem. Ref. Data **12**, 592 (1979).
[52]B. T. M. Willis, Nature (London) **197**, 755 (1963); Acta Crystallogr. Sect. A **34**, 88 (1978).
[53]N. Masaki and K. Doi, Acta Crystallogr. Sect. B **28**, 785 (1972); **24**, 1393 (1968).
[54]B. O. Loopstra, Acta Crystallogr. **17**, 651 (1964).
[55]D. Hall, A. D. Rae, and T. N. Waters, Acta Crystallogr. **19**, 389 (1965).
[56]V. M. Vdovenko, E. V. Stroganov, and A. P. Sokolov, Sov. Radiochem. **9**, 123 (1967).
[57]D. Petitmaire, J. Petiau, G. Calas, and A. M. Heron (unpublished).
[58]G. S. Knapp, B. W. Veal, D. J. Lam, A. P. Paulikas, and H. K. Pan, Mater. Lett. **2**, 253 (1984).
[59]G. Chauvet and R. Baptist, Solid State Commun. **43**, 793 (1982).
[60]P. J. Kelly and M. S. S. S. Brooks, Physica **102B**, 81 (1980).
[61]F. Gerken and J. Schmidt-May, J. Phys. F **13**, 1571 (1983).
[62]I. Davoli S. Stizza, A. Bianconi, M. Benfatto, C. Furlani, and V. Sessa, Solid State Commun. **48**, 409 (1984).
[63]G. Kaindl, G. Kalkowski, W. D. Brewer, E. V. Sampathkumaran, F. Holtzberg, A. Schach, and V. Wittenan, J. Magn. Magn. Mater. **47&48**, 161 (1985).
[64]R. C. Karnatak, M. Gasgnier, H. Dexpert, J. M. Esteva, P. E. Caro, and L. Albert, J. Less Common Met. (to be published).
[65]A. F. Leung, J. Phys. Chem. Solids **43**, 467 (1982).
[66]D. E. Perry, L. Tsao, and H. G. Brittain, J. Inorg. Chem. **23**, 1232 (1984).
[67]C. Keller and C. K. Jorgensen, Chem. Phys. Lett. **32**, 397 (1975).